

FOS-based Monitoring of underwater port structures

Annette SCHEIDER, Eike BARNEFSKE and Harald STERNBERG, Germany

Key words: Deformation measurement, structural health monitoring, geo sensor network, underwater structure, time series analysis

SUMMARY

In order to ensure the safe operation of critical infrastructure facilities like docks, the structural condition of quay facilities is monitored and documented through regular inspections and monitoring measurements. While geodetic monitoring systems for above-water structures are standard solutions, only a few sensor types are available for monitoring underwater structures. For that purpose, a measurement system is investigated which includes underwater inclinometers and fiber-optic Bragg grating strain sensors. Combined as a geodetic sensor network, they are mounted on one quay wall in the Port of Hamburg. The sensors acquire and record data as time series in order to show subsequently the deformation behavior of the wall. In addition, environmental parameters such as water level and temperature are recorded. Based on the measured data, the characteristics of the time series are investigated by methods of time series analysis (e.g. correlation analysis, Fast Fourier Transformation) to describe the interaction between potential influencing forces and geometric values. The suitability of the used sensors and analysis methods is evaluated and the deformations are modelled.

FOS-based Monitoring of underwater port structures

Annette SCHEIDER, Eike BARNEFSKE and Harald STERNBERG, Germany

1. MOTIVATION AND INTRODUCTION

A major part of the global transport is carried by ships. Delays in loading and unloading the ships have a negative impact on the global circulation of goods. One influencing factor in this process is the equipment and condition of the port facilities. Their full functionality is essential. If functional failures occur in quay systems that are generally exposed to various forces (e.g. current, shocks, load from cargo), this can severely disrupt cargo logistics. The recalculation of sheet pile walls is a challenge for classical static methods, because for hydraulic structures many of the influencing variables are unknown (Heins & Pucker, 2019). On older quay walls, a deformation monitoring system is recommended to determine its real status.

For this purpose, the suitability of different sensors for use in such a monitoring system is investigated and the observations are analyzed. In contrast to land-based systems, only a limited number of sensors are suitable to monitor underwater structures. They must either be installed directly in the relevant components of the structure or mounted on the considered wall surface in the water. Previous investigations from Del Grosso et al. (2007) describe a general concept for deformation monitoring on quay walls.

In this paper the realization of monitoring system and the modelling of the deformations is described. A geodetic sensor network (GeoSN) is developed for a quay wall in Hamburg. Fiber optic strain sensors (FOSG) and underwater inclinometer (UWI) are mounted on the waterside of a sheet pile wall of the quay wall. The focus is the investigation and the evaluation of those sensors. In addition, an elastic cause-effect model for the inclinations and strains is developed. The water level and the temperature are the main influences on this model.

2. DEFORMATION MONITORING OF UNDERWATER STRUCTURES

The state of the art for monitoring systems and the object of investigation, the quay wall, are briefly explained.

2.1 State of the art and technology

The development and operation of GeoSN is an active application and research field in geodesy. GeoSN are mostly used for monitoring constructions (Engel et al. 2018) or natural objects (Schönberger et al. 2020) and consist of individual sensors that measure geometric and non-geometric quantities, at specific locations on the object to be monitored (Schwieger & Sternberg, 2014). The measured values describe the current state of the object. This can be the temperature of the object surface, the height of the water level in the environment, the extension of the object, and many more. Based on these values, changes of the object properties can be measured and monitored directly. If only statements about occurring changes are to be made based on collected measured values, then a congruence model is set up from the monitoring data (Heunecke et al. 2013). This congruence model can be extended to a kinematic model if data is to be analyzed over a longer period and predictions about the future trend are met. In addition to analyzing the geometric influence, the non-geometric measured values can also be

investigated with regard to possible causal relationships (dynamic model). If causal relationships exist or respectively if there is a correlation between measured values, a dynamic model can be set up (Heunecke et al. 2013). The underlying model can be used to determine the quality of the measured values.

Newer GeoSN consist of a large number of sensors, which can no longer be displayed, managed, and analyzed in tables and 2D visualizations in a target-oriented manner. There are different users who focus on different information derived from the values. Database servers and a task-appropriate user interface must be developed (Jo et al. 2018). For complex structures such as bridges or tunnels, a digital twin (Wenner et al. 2021) or abstract model of the structure (Buchmayer et al. 2021) is mapped in which the sensors are represented true to location.

2.2 Investigated quay wall

The quay wall in Hamburg's bulk port has a length of about 700 m and consists of 26 blocks. Each block consists of a honeycomb sheet pile wall and two supporting piles at the block edges. The quay wall has a total height of about 32 m including the quay platform. About 10 m are part of the foundations. The remaining 22 m of the quay wall are subjected to different loads from the waterside, depending on the water level and port operations. At mean high water (MHW), about 17 m of the quay wall are covered with water and 5 m are above the water line (Figure 1).

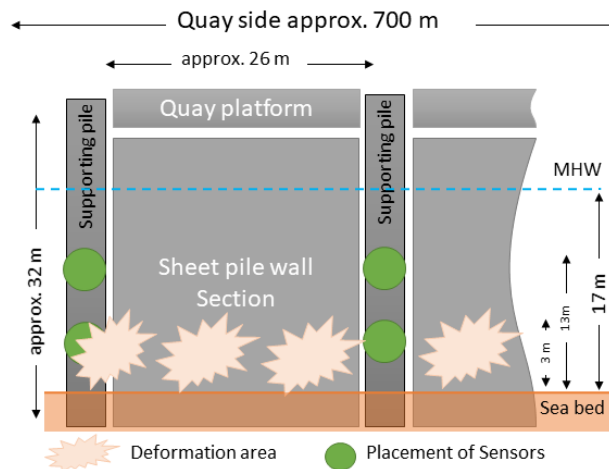


Figure 1: Layout of the quay wall under monitoring with the areas of previously occurred deformations and the placements of the sensors.

The quay wall is monitored from land and water side in intervals. During these monitorings, major deformations were detected at some spots. Actions for securing were initiated. Since a quay wall in port operations is affected by a large number of known and unknown influences, static simulation are a weak approximation. In order to support the static model the quay wall is equipped with geometric sensors to monitor permanently with a high-resolution. The sensors are installed at a height of 3 m and 13 m above ground (Figure 1). Deformations occur at the height of approx. 3 m and it is supposed that there is no significant deformation at the height of 13 m. In addition to the sensors for geometric deformations, tide gauge and thermometers are installed.

3. MONITORING CONCEPT

3.1 Sensor Technology

Inclination angles and wall strains at certain positions describe the deformation of the quay wall. The monitoring system is installed on an existing quay wall and the performance of post installed UWI, FOSG and extensometers are investigated.

2.1.1 Underwater Inclinometer

The UWI are mounted in areas with occurring deformations und other areas which are expected to be stable (green dots in Figure 1). They determine the vertical inclination of the supporting pile. The UWIs have two sensitive axis and a resolution of 0.02 mm/m. They consist of classical building inclinometer (Möser et al. 2016) placed in a water proof housing. The manufacturer specifies the linearity of the measured values as 0.2 % f.s. for $\pm 5^\circ$. Compared to a smoothed time series, the root mean square (RMS) of all UWIs is in a range of 0.014 mm/m and 0.021 mm/m. Each UWI is equipped with a temperature sensor. It can be deployed within a temperature range of -25°C up to 85°C . This is used to compensated errors caused by the temperature change.

2.1.2 Fiber-optical strain gauge

FOSG base on the physical principle that light waves of a certain wavelength are (totally) reflected while passing an area with different refractive indices (Figure 2). FOSG are used to measure strain changes at discrete locations (e.g. fiber Bragg grating (FBG)SG) or along a structure (e.g. continuous fibers (CF)). Since the strain in a local area is of interest, the FBGSGs will be used. FBGSG use a Bragg grating etched into the fiber at discrete locations. The Bragg grating acts like an optical filter that reflects a certain wavelength range of the emitted light (Bragg frequency) and allows the other light waves to pass (Pfeiffer, 2000). The grating spacing (Λ) determines which wavelength range λ_B is reflected and (1) is used to calculate the reflected Bragg wave (Pfeiffer 2000).

$$\lambda_B = 2 * \Lambda * n \quad (1)$$

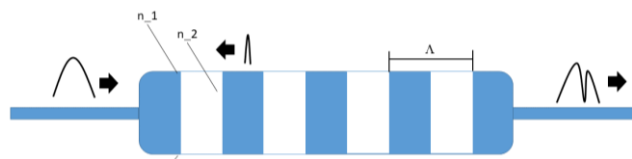


Figure 2: The principle of the FBG SG with the parameters refractive index (n) and grating spacing (Λ).

The lattice spacing and the refractive index change due to temperature changes and mechanical influences. If the temperature change is known, the mechanical strain can be determined by means of the wavelength change (Tosi 2017).

2.1.3 Extensometers

Due to the varying load on the wall, there is also a concern that a base failure (Kolymbas 2016) may occur. Rod extensometers are installed behind the quay wall in order to detect earth movements and resulting vertical displacements (change in length) early. Four sensors are fixed in depth intervals of 3 m at each measurement point. According to the manufacturer, the accuracy is approx. 0.02 mm. The measuring principle of extensometers is explained e.g. by Möser et al. (2016).

2.1.4 Environmental sensors

In order to acquire potential influencing parameter water level reps. water pressure, two water level probes (tide gauges) are installed. They have a measurement range of more than 1 bar. The manufacturer specifies a long-term drift of 0.1% and a maximum measurement accuracy of 1%. One probe is mounted front of the quay wall and another is installed in a shaft behind the quay wall. Here, the empirical standard deviation is 1.3 cm or resp. 0.7 cm. The water level probes are also completed by a temperature sensor to compensated the errors from temperature change.

3.2 **Realization of the monitoring system**

The GeoSN can be divided into three sections. The first section are the sensors at the quay wall (Figure 1), the second section is the transmission and the control unit on site and the third section is the data evaluation and the use by external users (Figure 3).

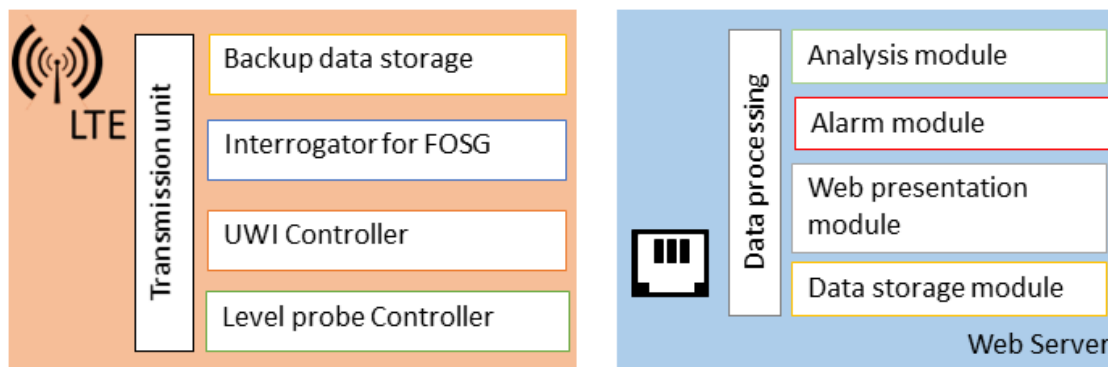


Figure 3: Realised Monitoring system.

The first section is the secure and water resistance installation of the sensors and wired signal transfer to the control unit that links the GeoSN to the internet (Figure 1). Seven FOSG are arranged above and beyond the upper UWI. They are named FOSG 1 to FOSG 7 from top left to bottom central. FOSG 2 and FOSG 7 are aligned horizontally while all other FOSG sensors have a vertical alignment (sensitive axe).

The transmission and control unit are in the flood protected area and consists of an interrogator for the FOSG, a control unit for the UWI, a database for all collected measurement data and an LTE module for data transmission to a web server. As the GeoSN executes multiple evaluation steps and methods independently and simultaneously. The software is designed in such a way that the modules can be switched on and off at any time and that new modules can be added

during operation. The central modules of the web server are the data storage, the visualization in a user-specific web portal, the analysis and further processing of the data, as well as the alerting in case of failures or remarkable changes in the measurement data (Figure 3).

4. DEFORMATION ANALYSIS

4.1 Time series analysis

The different effects influencing the measured inclinations include drift effects, cyclical effects and further deterministic correlations. Therefore, their behaviour can only be described functionally after applying methods of time series analysis. For this purpose, the measurement data recorded by the different sensors are treated as discrete time series with a recording interval of 60 s. In the time series analysis, measurement data collected over an observation period of nearly two month are investigated as an example. Due to a malfunction, the data of the level probe are only available for approx. one months. Outliers are removed from the time series. For the considered time series of FOSG measurements, a compensation of the temperature influence has already been performed. But they still contain numerous discontinuities of varying magnitude. Some of these are individual outliers or sudden changes of their mean values (jumps) in the data series. As exsample, some FOSG show variations and jumps during the first four days. The first days are considered as a run-in phase and are not taken into account for the time series analysis. It has to be considered, that the measured strains are damped by the adapter plates. This effect was investigated and explained by Barnefske et al. (2020).

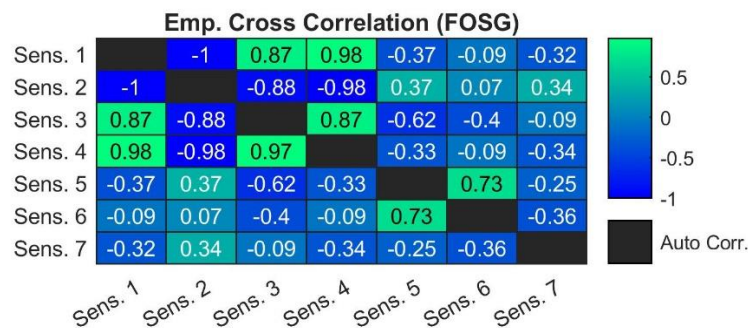


Figure 4: Empirical Cross Correlations coefficients $\hat{C}(0)$ between time series of the FOSG sensors 1-7

Due to the large strains in the object, over-stretchings occur in some FBGs and finally lead to a fibre break at all sensors after a measurement duration of 6 month. A time intervall of approx. 2 month is analyzed containing different effects and influences. The empirical cross-correlation coefficients between the trend-adjusted time series of all FOSG sensors are determined in order to be able to look at the influence of these events in more detail. Figure 4 shows the empirical cross correlation ($\hat{C}(0)$). There is a high similarity between the data of the FOSG 1 to 4, which are mounted above the UWI. The absolute cross correlation coefficients are 0.88 and higher. The high magnitude of the data jumps at the beginning of time series of FOSG 2 and its correlation coefficient of -1 compared to the decoupled sensor FOSG 1 even might indicate the detachment of a weld on the mounting plate of FOSG 2. Additionally, the $\hat{C}(0)$ coefficients between the data of the neighbouring FOSG 5 and 6 as well as FOSG 3 and 5 reach 0.73 or

- 0.62 respectively. Since the time series of FOSG 7 contains multiple discontinuities like data jumps (max. magnitude 0.64 mm/m), this distorts the result of the $\hat{C}(0)$ analysis and the determined absolute $\hat{C}(0)$ coefficients are always less than 0.37.

In order to consider the periodic effects of the time series, the general trend is reduced in the time series. The analysis of the high-pass filtered and reduced time series is performed with a Fast Fourier Transformation (FFT). The results show clearly a dominating frequency of approx. $2.263 \cdot 10^{-5}$ Hz for tide gauge data as well as for the measured inclinations and strain. The corresponding wavelength of 12 h and 16 min refers clearly to the occurring tidal variation of the water level. However, the empirical cross correlation between the filtered time series of the tide gauge and the FOSG is small (≤ 0.22) for most of the sensors. Probably, this result is caused by the included data jumps as well as by the shape of the occurring periodic effects in the different time series of the FOSGs (Figure 5). Additionally, sudden amplitude changes also affect this result. Besides, the transmission behavior of the influence parameter on the deformation parameters is not necessarily linear. As an exception, the corresponding correlation coefficients of FOSG 3 and 7 are slightly higher (FOSG 3: -0.54, FOSG 7: 0.29). The time series of the sensor FOSG 7 represents a special case. It contains periodic effect with an amplitude of approx. 0.02 mm/m which is higher than in other time series. The sensor seems to have detached from the wall and shows a behavior that is obviously influenced by the tide.

The empirical $\hat{C}(0)$ coefficient between the neighbouring UWI and tide gauge is -0.76 with a small lag of 5 minutes. Generally, the amplitudes of the UWI installed 3 m above ground are higher than the upper ones. Here the exaggeration factor is 1.9.

Analysing these effects by Short Time Fourier Transformation (STFT), which is shown by Kiencke et al. (2008), confirms the dominating effect of the detected frequency. However, it also shows that the amplitude of the periodic effect is not equal for the complete time series. Looking more closely at the periodic effects, it is apparent that the FOSG do not reflect water level fluctuations as clearly as the UWI data. The data include more noise and the amplitude is lower. Changes in the water temperature dominantly affect the measured UWI values, which indicates the necessity of a consideration of further dependencies. In this case, the $\hat{C}(0)$ coefficients between the data are sensor dependent. For the considered sensors, the coefficients are -0.36 (upper UWI) or respectively -0.52 (lower UWI).

In addition, the relationships between longer-term water level fluctuations and the observed strains are also determined by comparing the low-pass filtered parts of the time series. The empirical $\hat{C}(0)$ between the FOSG and the tide gauge data reach empirical $\hat{C}(0)$ coefficients of 0.33 for FOSG 2 and 0.42 for FOSG 7 for the horizontally mounted sensors. The $\hat{C}(0)$ calculated for all vertically aligned FOSG are in a range of -0.27 to 0.14. Here, only sensor FOSG 3 has a positive $\hat{C}(0)$ coefficient because other effects than the tidal effect are more dominant in this time series.

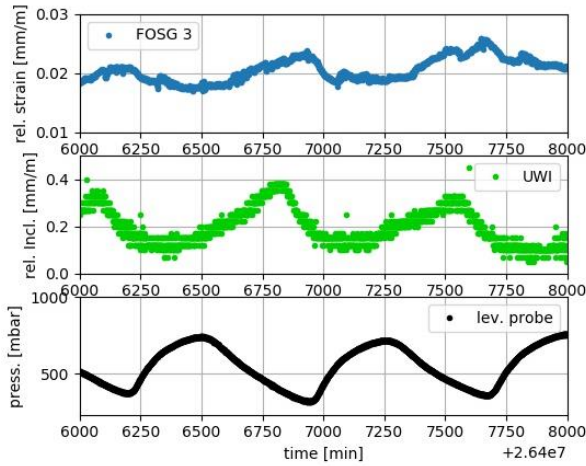


Figure 5: Segment of the time series of FOSG 3 (blue), UWI (green) and tide gauge (black).

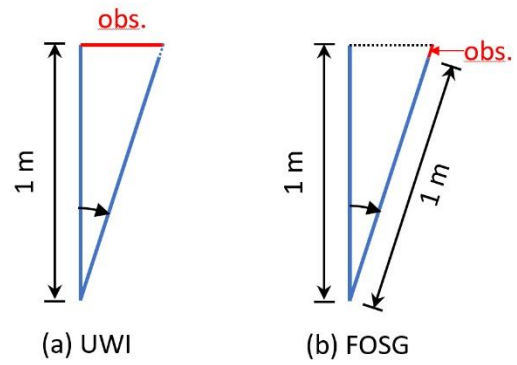


Figure 6: Measured variables – (a) UWI: inclination, (b) FOSG: strain.

Interpreting the given inclination as a leg of a right-angled triangle, the corresponding strain is approx. by comparing the length of the hypotenuse to the base length of 1 m (Figure 6). These are compared to the trend-reduced time series of the FOSG. The empirical cross correlation coefficient ($\hat{C}_{UWI,FOSG}(0)$) is used to express the similarity between different sensors in the GeoSN. The $\hat{C}_{UWI,FOSG}(0)$ between UWI and the surrounding FOSG vary strongly (Table 1). For FOSG mounted above the UWI, the absolute $\hat{C}(0)$ coefficients are 0.80 or larger. The recorded inclinations probably are caused mainly by a bending of the wall itself. In contrast, FOSG 5 to FOSG 7 show little similarity to the UWI data. The $\hat{C}_{UWI,FOSG}(0)$ coefficients are smaller than 0.42. Eventually, the FBGs in FOSG 5 and FOSG 6 were over-stretched at the beginning of the measurements and do not provide reliable measurements for the majority of the considered time interval.

Table 1: Empirical cross correlation coefficients $\hat{C}_{UWI,FOSG}(0)$ between UWI and the individual FOSG sensors. Due to data gaps, the value with * cannot be calculated over the entire measurement sequence.

| | $\hat{C}_{UWI,FOSG}(0)$ |
|--------|-------------------------|
| FOSG 1 | -0.83 |
| FOSG 2 | 0,77* |
| FOSG 3 | -0.82 |
| FOSG 4 | -0.80 |
| FOSG 5 | -0.42 |
| FOSG 6 | -0.12 |
| FOSG 7 | -0.00 |

A further potential influence is earth mass displacements behind the quay wall itself. They might be detected by changes in the extensometer time series. Even these data are affected by tidal influences. The contained periodic effects have a dominating frequency of $2.255 \cdot 10^{-5}$ Hz. Only the top extensometer element is dominated by an approximate diurnal

cycle with a frequency of $1.1285 \cdot 10^{-5}$ Hz. Generally, this cyclic effect occurs with a delay of more than 2 h compared to the water level variations. The time series of the extensometers are affected by data jumps but also by continuing variations of the mean value. The long-term changes of the mean value are significantly smaller than 1 mm. In order to investigate the dependency between the measured displacements and the inclinations without consideration of the tidal influence, the empirical cross correlations are computed for the low-pass filtered part of the time series only. Since an extremal cross correlation is only reached after at least one day, it can be supposed that there is only an indirect correlation via the (unknown) groundwater level.

4.2 Modelling of deformations

Different forces influence the deformation behaviour of quay walls. For example, water level changes, or precisely the change of water pressure, are assumed to be an important acting force. In the considered case, a periodic deformation is mainly caused by the tidal variations of the water level. Next to this and other acting forces (e.g. earth mass displacement behind the wall) or respectively the occurring deformations, the measurements are also affected by a potential drift behaviour of the sensors.

In order to describe the available time series by potentially influencing parameters (water pressure and temperature), static and dynamic models are investigated to describe the varying inclinations for two sensor placements lying upon each other. Additionally, the models are also applied to the time series of the FOSG sensors.

The modelled deformations for the individual inclinations and strains are considered based on a multiple regression analysis in dependence from the (discrete) acquisition time t_k , the water pressure p and the corresponding water temperature T . Displacements measured by the extensometers are not contained in the model. In order to express the behaviour with a simple dynamic model, four approaches are considered.

Polynomial models:

$$f_1(T, p) = a_{01} + b_{12} \cdot T(t_k) + b_{22} \cdot (T(t_k))^2 + c_{12} \cdot p(t_k) + c_{22} \cdot (p(t_k))^2 \quad (2)$$

$$f_2(T, p) = a_{02} + a_{12} \cdot t_k + b_{12} \cdot T(t_k) + b_{22} \cdot (T(t_k))^2 + c_{12} \cdot p(t_k) + c_{22} \cdot (p(t_k))^2 \quad (3)$$

Differential models:

$$f_3(T, \dot{T}, p, \dot{p}) = a_{03} + b_{13} \cdot T(t_k) + b_{23} \cdot \dot{T}(t_k) + c_{13} \cdot p(t_k) + c_{23} \cdot \dot{p}(t_k) \quad (4)$$

$$f_4(T, \dot{T}, p, \dot{p}) = a_{04} + a_{14} \cdot t_k + b_{14} \cdot T(t_k) + b_{24} \cdot \dot{T}(t_k) + c_{14} \cdot p(t_k) + c_{24} \cdot \dot{p}(t_k) \quad (5)$$

where t_k = time at epoch k ,
 T = measured temperature,
 \dot{T} = Temperature change,
 p = measured water pressure,
 \dot{p} = change of the water pressure.

For each model, $i = (1,2,3,4)$, the regression coefficients a_{0i} to c_{2i} are determined and applied to model the sensors' behaviour.

Table 2: RMS of the deviations between UWI data and modelled inclinations for Eq. (1) – Eq. (4)

| | Upper UWI | Lower UWI |
|----------------|------------|------------|
| Eq. (2) | 0.084 mm/m | 0.039 mm/m |
| Eq. (3) | 0.106 mm/m | 0.663 mm/m |
| Eq. (4) | 0.097 mm/m | 0.044 mm/m |
| Eq. (5) | 0.045 mm/n | 0.044 mm/m |

Here we first consider two inclinometers attached to one support pile of the wall (Figure 1). The deviations between the different modelled inclinations (2) to (5) and the particular UWI time series are summarized in Table 2 as Root Mean Square (RMS) values. The minimal RMS value is 0.039 mm/m for modelling the time series of the lower UWI with (2). This time series can also be modelled quite well by the differential models (4) and (5) with a RMS of 0.044 mm/m. For the upper UWI, a comparable RMS value (0.045 mm/m) can only be reached for the differential model according to (5). It indicates, that a time dependent drift behaviour is included in the time series.

Table 3: RMS of the deviations between exemplary FOSG data and modelled strains for Eq. (2) – Eq. (5).

| | FOSG 1 | FOSG 3 | FOSG 4 | FOSG 5 | FOSG 7 |
|----------------|------------|------------|------------|------------|------------|
| Eq. (2) | 0.014 mm/m | 0.174 mm/m | 0.014 mm/m | 0.005 mm/m | 0.093 mm/m |
| Eq. (3) | 0.014 mm/m | 0.174 mm/m | 0.012 mm/m | 0.794 mm/m | 0.581 mm/m |
| Eq. (4) | 0.020 mm/m | 0.282 mm/m | 0.015 mm/m | 0.005 mm/m | 0.095 mm/m |
| Eq. (5) | 0.014 mm/m | 0.174 mm/m | 0.012 mm/m | 0.804 mm/m | 0.592 mm/m |

Due to data gaps in the different involved data sets, the time series of the FOSG sensors can only be approximated for a time interval of 30 days. The included outliers are eliminated. Because of the high absolute empirical cross correlation coefficient between the time series of FOSG 1 and 2 (Figure 4), there is no additional model for FOSG 2 in this comparison. Caused by the contained effects (e.g. discontinuities, strong noise), it is hardly possible to approximate the FOSG 3 and FOSG 5 to 7 time series by the defined models (2) to (5). For this reason the RMS values shown in Table 3 are generally more than factor 4.6 larger than those of FOSG 1 and FOSG 4. But even here, certain components of the time series can not be modeled completely and absolute deviations of up to 0.03 mm/m occur (Figure 8). Especially the strong signal increase in the considered period can only be approximated to a limited extent by the influencing variables used here.

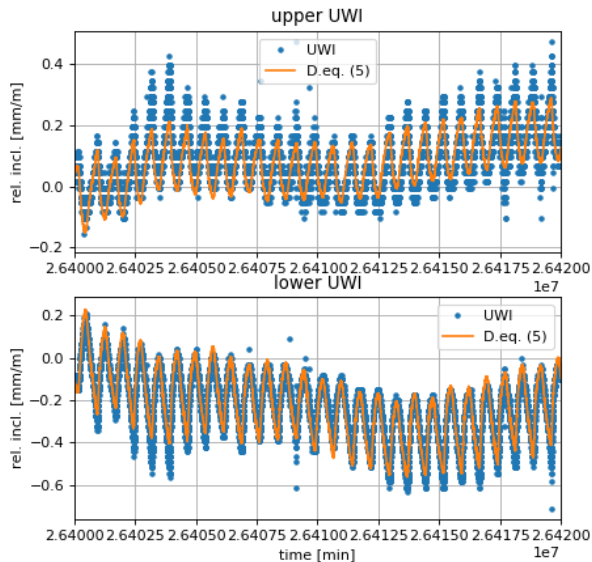


Figure 7: Relative Inclinations of the upper and the lower UWI on the supporting pile, modelled by equation (5).

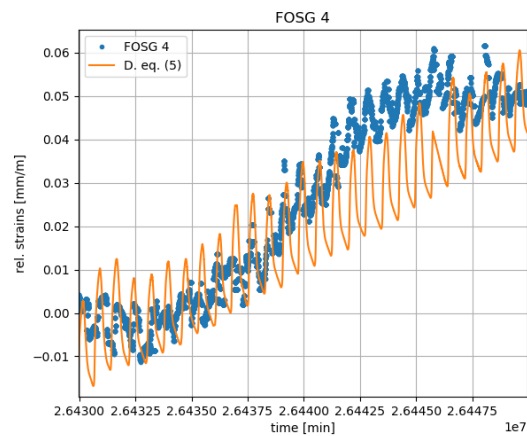


Figure 8: Relative strains of the FOSG 4 sensor, modelled by equation 5.

Comparing all results in Table 2 and Table 3, the model (5) is preferable for the time series under consideration, even if it is not able to describe or explain all occurring effects. This is clearly shown in the upper part of Figure 7 and Figure 8. The occurring amplitude of the varying inclinations cannot be modelled here. This is possibly because the model only describes the inclinations and strains in dependence to environmental factors. Therefore it can only partly predict future deformations. For a more comprehensive modelling further influencing variables have to be measured. These are the load on the quay or the groundwater level could be integrated for this purpose.

5. CONCLUSION AND OUTLOOK

The behaviour of the quay wall is partly influenced by the water level. This is confirmed by the detected empirical cross correlations of -0.76 for UWI. The dependency between FOSG sensors and the water level variations is not so obvious, here $|\hat{C}_0| < 0.42$ for the horizontally aligned sensors and $|\hat{C}_0| < 0.27$ for the vertically aligned FOSG. Additionally, the water temperature affects the measured values to a certain extend. The influence of the temperature is mainly compensated by measurements with temperature sensors. A complete compensation cannot be guaranteed due to the measurement setup. Also, the steel of the wall changes with temperature changes, so that the temperature change can lead to mechanical strain. In addition, the FOSG time series show attenuation of the included effects compared to the UWI.

The investigations show that a GeoSN can also be attached to existing quay walls for monitoring purposes. If one generally considers the quality of the data of the measurement data in the GeoSN, different quality characteristics or criteria are to be defined (Wiltschko, 2004). This are for example, availability, reliability, correctness, consistency, and geometry.

In principle, UWIs are very well suited for the considered task. Although no statement can be made about the correctness of the measurement data with this prototype, sufficient (geometric) accuracy can be determined at each sensor. The measurement noise is in the range of the

resolution of 0.02 mm/m. The data are consistent. However, the availability is not 100% yet. It is recommended to add the GeoSN by a tide gauge because tidal variations of the water level affect the detected inclinations. The installation of further UWIs in the individual blocks will enable to calculate deflection curves and their deformations. The availability and the reliability of the FOSG measurements in this experiment was lower compared to the UWI. While most of the UWIs continued in data registration for the complete project duration of 1 year, the FOSG failed after six months. The most probable reason is disrupted fibre. In addition, sudden data jumps that could cause by installation decrease the reliability and the correctness of the data. Shortly before the fibres are overstretched, a strong measurement noise occurs in the measurement data that reduces the accuracy.

Nevertheless, the costs for a dense FOSG GeoSN are lower compared to GeoSN of UWI. Therefore, it can be distributed all over the object and a higher sensor density can be realized. This leads to a better spatial resolution so the measured strains would even contain local deformation effects. In the case of future installation on existing underwater objects, the mounting of the FOSG must be optimized and distributed FOSG, such as by Buchmayer et al. 2021, should be used. More Prior knowledge about the deformation behaviour need be considered to optimize the FOSG with a measuring range. In addition, the fibre must be protected against damage (especially during attachment). The FOSG can generally be used for measurements under water without any restrictions (electromagnetic immune). Only the interrogator must be installed at water-protected and dust-free place. However, the installation of the sensors on existing constructions and the replacement of defective sensors (FOSG and UWI) is very costly.

Before the installation of a GeoSN, the transfer behaviour between sensors' output and known influencing factors should be determined in more extensive experiments (e.g. in climate chamber). In addition, the damping effect of the adapter plates of the FOSG have to be further investigated. Alternatively, other installation techniques are required, even if they more complex and costly.

ACKNOWLEDGEMENT

The authors want to thank the Hamburg Port Authority for this project. Special thanks go to our direct contacts Rico Priewe (Hamburg Port Authority) and Bernd Löden who started the project, introduced us to the structure of the quay wall and realized the monitoring system. Our thanks also go to the members of the project team, Güren Dinga (HCU) and Janek Stoeck (formerly HCU) for their work in developing the database and the web interface as well as their investigations.

REFERENCES

- Barnefske, E., Ohlendieck, J. & Sternberg, H. (2020). Modellierung der Deformation eines Stahlträgers durch indirekte Dehnungsmessungen. In: *Tagungsband GeoMonitoring 2020*. Gerke, M. & Riedel, B. (eds.), TU Braunschweig, pp. 93-103.
- Buchmayer, F., Monsberger, C. M. & Lienhart, W. (2021). Advantages of tunnel monitoring using distributed fibre optic sensing. *Journal of Applied Geodesy*, Vol. 15, No. 1, pp. 1-12. <https://doi.org/10.1515/jag-2019-0065>

- Del Grosso, A., Lanata, F., Brunetti, G. & Pieracci, A. (2007). Structural health monitoring of harbour piers. *SHMII-3 2007*, Vancouver, British Columbia, Canada.
- Engel, P., Foppe, K. & Köster, U. (2018). Multi-Sensor-System zur Erfassung von Turmschwingungen an der Marienkirche Neubrandenburg. In: *MST 2018 – Multisensortechnologie: Low-cost im Verbund*, Beiträge zum 176. DVW-Seminar am 13. und 14. September in Hamburg, Wißner Augsburg.
- Heins, E. & Pucker T. (2019). Zur Anwendung numerischer Verfahren bei der Berechnung von Ufereinfassungen im Bestand. Bundesanstalt für Wasserbau, Kolloquium Numerik in der Geotechnik, 9. und 10. Oktober 2019 in Karlsruhe.
- Heunecke, O., Kuhlmann, H., Welsch, W., Eichhorn, A., & Neuner, H. (2013). Auswertung geodätischer Überwachungsmessungen. *Handbuch Ingenieurgeodäsie*, Möser, M., Müller, G., Schlemmer, H. (eds), 2, Wichmann Verlag, Berlin Offenbach.
- Jo, B. W., Jo, J. H., Khan, R. M. A., Kim, J. H., & Lee, Y. S. (2018). Development of a Cloud Computing-Based Pier Type Port Structure Stability Evaluation Platform Using Fiber Bragg Grating Sensors. *Sensors*, Vol. 18, No. 6, Art.-No. 1681, <https://doi.org/10.3390/s18061681>
- Kiencke, U., Schwarz, M. & Weickert, T. (2008). *Signalverarbeitung - Zeit-Frequenz-Analyse und Schätzverfahren*. Oldenbourg München.
- Kolymbas, D. (2016). *Geotechnik – Bodenmechanik, Grundbau und Tunnelbau*. 4, Springer Vieweg Berlin.
- Möser, M., Müller, G. & Schlemmer, H. (eds) (2016). *Handbuch Ingenieurgeodäsie – Ingenieurbau*. 2, Wichmann Berlin Offenbach.
- Pfeiffer, F. C. (2000). Einfluß ionisierender Strahlung auf die Funktionsfähigkeit faseroptischer Bragg-Gitter-Sensoren, PhD, Gerhard-Mercator-Universität Duisburg.
- Schönberger, C., Lienhart, W., Lang, E. & Stary, U. (2020): Erfahrungen aus 20 Jahre GPS Monitoring der Massenbewegung Gradenbach. In: *Tagungsband Geomonitring 2020*, pp. 149-162. DOI: <https://doi.org/10.15488/9347>
- Schwieger, V. & Sternberg, H. (2014). Multi- Sensor-Systeme in der Ingenieurgeodäsie – Grundlagen und Überblick. In: *Multi-Sensor-Systeme – Bewegte Zukunftsfelder*. Beiträge zum 138. DVW-Seminar am 18. und 19. September in Hamburg, Band 75/2014, Wißner Augsburg, pp. 3-23.
- Tosi, D. (2017). Review and analysis of peak tracking techniques for fiber Bragg grating sensors. *Sensors*, Vol. 17, No. 10, Art.-No. 2368, pp. 2368-2403, <https://doi.org/10.3390/s17102368>
- Wenner, M., Meyer-Westphal, M., Herbrand, M. & Ullerich, C. (2021). The Concept of Digital Twin to Revolutionise Infrastructure Maintenance: the Pilot Project smartBRIDGE Hamburg, In *27th ITS World Congress*, Hamburg, Germany, 11-15 October 2021.
- Wiltshko, T. (2004). Sichere Information durch infrastrukturgestützte Fahrerassistenzsysteme zur Steigerung der Verkehrssicherheit an Straßenknotenpunkten. Phd, University of Stuttgart. VDI Verlag, Düsseldorf, Germany.

BIOGRAPHICAL NOTES

Dr.-Ing. Annette Scheider is head of the geodetic laboratory at HafenCity University Hamburg since 2018. Between 2010 and 2018 she was a research associate at University of Stuttgart. She is a member of the DVW, of the DVW working group 8 (Mobile and Autonomous Sensor Systems) and the DHyG.

M. Sc. Eike Barnefske is a research assistant at HCU since 2016. Since 2017, he is a member of the Hydrography and Geodesy group. He is a member of the DVW.

Prof. Dr.-Ing. Harald Sternberg is professor for Hydrography and Geodesy at the HafenCity University Hamburg since 2017, before that he was professor for Engineering Geodesy and Geodetic Metrology since 2001. Beside his research activities in the area of hydrography, indoor navigation and data-driven analysis, he was the vice president for teaching and studies at the HCU for 13 years. He is a member of the DVW (in the past he has chaired the Multi-Sensor-Systems working unit) and of the DHyG, and was delegated to the IBSC (FIG/IHO/ICA international board on standards of competence for hydrographic surveyors and nautical cartographers) by the FIG.

CONTACTS

Dr.-Ing. Annette Scheider, M.Sc. Eike Barnefske and Prof. Dr.-Ing. Harald Sternberg
HafenCity University Hamburg
Henning-Voscherau-Platz 1
20457 Hamburg
GERMANY
Tel. +49 40 42827 4546
Email: annette.scheider@hcu-hamburg.de,
eike.barnefske@hcu-hamburg.de and harald.sternberg@hcu-hamburg.de